Path-following funnel control for rigid-link revolute-joint robotic systems

T. Faulwasser[†] and C.M. Hackl[⋆,‡]

***Abstract*— In this paper we investigate the application of funnel control to unconstrained path-following problems. While funnel control is a high-gain based time-varying feedback strategy applicable to minimum-phase systems with known relative degree, path following refers to the problem of tracking a reference path in an output space. A particular feature of path following is that the timing along the reference path is not determined a priori. The timing is adjusted online by the controller and may be exploited to improve the tracking performance. We show that the combination of funnel control and path following is applicable to fully-actuated rigid-link revolute-joint robots.**

I. Introduction

Usually, one distinguishes the control problems of set-point stabilization and trajectory tracking. While the former refers to the task of stabilizing a feedback system around a point in state space, the latter describes the design of controllers which ensure tracking of time-varying references. However, not all control problems fit into this framework. For instance, consider the task to steer a robot along a pre-specified (prescribed) geometric curve in its workspace (or the corresponding joint space), whereby the speed to move along the curve is not fixed a priori. Such problems are usually referred to as path-following problems, see [1]–[3].

Different approaches to solve path-following problems are discussed in the literature: In [1], [2] and [4], [5] backstepping, respectively, geometric control are considered. In [3], [6], [7] tailored predictive control schemes are presented. In the present contribution, we investigate the application of funnel control to path-following problems of rigid revolute-joint robotic systems.

Funnel control—developed by Ilchmann et al. (see e.g. [8]–[11] and references therein) for systems with bounded-input bounded-output (BIBO) stable zero-dynamics, known relative degree and known sign of the high-frequency gain—is a high-gain based time-varying control strategy which guarantees *tracking with prescribed transient accuracy*, i.e. the absolute value of the control error (difference between regulated output and reference signal) is *limited* by a prescribed (possibly non-increasing) function of time.

In this contribution we will combine both methods. The combination of funnel control and path following assures that the path error (difference between regulated output and desired path) is always kept within prescribed bounds.

The remainder of this paper is organized as follows: In Section II we recall output path-following problems and introduce the considered class of robotic systems. In Section III we briefly re-visit funnel control for reference tracking of this system class. In Section IV we give sufficient conditions which allow to combine funnel control with path following. In Section V we apply path-following funnel control for position control of a planar (elbow-like) robot and present simulation results as a proof of concept.

Notation

$\mathbb{N}, \mathbb{R}, \mathbb{C}$	natural, real and complex numbers.
$[a, b)$	interval from a to b (excluded).
$\mathbb{R}_{>0},\ \mathbb{R}_{\geq 0}$	positive real numbers, with zero.
$\boldsymbol{x} \in \mathbb{R}^n, \mathbf{0}_n \in \mathbb{R}^n$	column, zero vector.
$\boldsymbol{A} \in \mathbb{R}^{n\times m}$	matrix with n-rows & m-columns.
$\det(\boldsymbol{A})$, $\operatorname{spec}(\boldsymbol{A})$	determinant, spectrum of $\boldsymbol{A} \in \mathbb{R}^{n\times n}$.
$\operatorname{diag}\{a_1, \ldots, a_n\}$	diagonal matrix with $a_1, \ldots, a_n \in \mathbb{R}$
$\boldsymbol{I}_n$, $\widetilde{\boldsymbol{I}}_n \in \mathbb{R}^{n\times n}$	$:= \operatorname{diag}\{1, \ldots, 1\}$, $:= \left[\begin{smallmatrix} \mathbf{0}_{n-1} & I_{n-1} \\ 0 & \mathbf{0}_{n-1}^\top \end{smallmatrix}\right]$
$\boldsymbol{f}(\cdot)$; $\boldsymbol{f}(t)$	a function $\boldsymbol{f}\colon I \subseteq \mathbb{R}_{\geq 0} \to Y \subseteq \mathbb{R}^n$, $n \in \mathbb{N}$; value of $\boldsymbol{f}(\cdot)$ at $t \in I$.
$\boldsymbol{f}^{(i)}(t) := \frac{\mathrm{d}^i}{\mathrm{d}t^i}\boldsymbol{f}(t)$	the i-th (time) derivative of $\boldsymbol{f}(\cdot)$ at t.
$\mathcal{C}^n(I; Y)$	space of n-times continuously differentiable functions mapping $I \to Y$.
$\mathcal{L}^p_{(\mathrm{loc})}(I; Y)$	space of measurable, (locally) p-integrable functions.
$\mathcal{L}^\infty_{(\mathrm{loc})}(I; Y)$	space of measurable, (locally) essentially bounded functions with norm:
$\lVert\boldsymbol{f}\rVert_\infty$	$:= \text{ess-sup}_{t\in I} \lVert\boldsymbol{f}(t)\rVert$.
$\mathcal{W}^{k,\infty}(I; Y)$	space of bounded locally absolutely continuous functions with essentially bounded derivatives $\boldsymbol{f}^{(i)} \in \mathcal{L}^\infty(I; Y)$ for all $i \in \{1, \ldots, k\}$.

II. Path-following problems

We consider nonlinear continuous-time, control-affine systems of the following form

$$\dot{\boldsymbol{x}} = \boldsymbol{f}(\boldsymbol{x}) + \sum_{j=1}^{n_u} \boldsymbol{g}_j(\boldsymbol{x}) u_j, \quad \boldsymbol{x}(0) = \boldsymbol{x}_0 \in \mathbb{R}^{n_x} \tag{1a}$$

$$\boldsymbol{y} = \boldsymbol{h}(\boldsymbol{x}), \tag{1b}$$

where $\boldsymbol{x} \in \mathbb{R}^{n_x}$ is the state, $\boldsymbol{u} \in \mathbb{R}^{n_u}$ is the input and $\boldsymbol{y} \in \mathbb{R}^{n_y}$ is the output (with dimensions n_x, n_u, $n_y \in \mathbb{N}$). Subsequently, we assume that the vector fields $\boldsymbol{f} : \mathbb{R}^{n_x} \to \mathbb{R}^{n_x}$, $(\boldsymbol{g}_1, \ldots, \boldsymbol{g}_{n_u}) : \mathbb{R}^{n_x} \to \mathbb{R}^{n_x \times n_u}$ and $\boldsymbol{h} : \mathbb{R}^{n_x} \to \mathbb{R}^{n_y}$ are sufficiently often continuously differentiable.

[⋆,‡] Corresponding author: C.M. Hackl is leader of the research group "Control of renewable energy systems (CRES)" at the Munich School of Engineering (MSE), Technische Universität München (TUM), Germany, christoph.hackl@tum.de

[†]T. Faulwasser is with the Laboratoire d'Automatique, École Polytechnique Fédérale de Lausanne, CH-1004 Lausanne, Switzerland timm.faulwasser@epfl.ch

In the present contribution we consider the problem of following a geometric curve

$$\mathcal{P} = \{\boldsymbol{y} \in \mathbb{R}^{n_y} \mid \theta \in \mathbb{R} \mapsto \boldsymbol{y} = \boldsymbol{p}(\theta)\} \tag{2}$$

in the output-space defined by (1b). The reference $\mathcal{P}$ is denoted as *path* and $\boldsymbol{p} : \mathbb{R} \to \mathcal{P}$ is called its parametrization. We assume that $\mathcal{P}$ is a regular curve [12] and that its parametrization $\boldsymbol{p}$ is sufficiently often continuously differentiable. The main idea of path following is that the timing—i.e. the map $t \mapsto \theta(t)$—is not determined a priori. Rather it is a degree of freedom and has to be calculated online in the controller. Formally, we consider the following control problem:

Problem 1 (Output path following)**.**
Given system (1a)*, reference path* $\mathcal{P}$ *as in* (2) *and prescribed function* $\psi_{i,0} : \mathbb{R}_{\geq 0} \to \mathbb{R}_{>0}$ *for* $i \in \{1, \dots, n_y\}$*, design* a feedback $\boldsymbol{u}$ and a timing θ *which achieve:*

i) ***Prescribed path accuracy****: The system output* $\boldsymbol{y} = \boldsymbol{h}(\boldsymbol{x})$ *converges such that forall* $t \geq 0$*:*

$$\forall i \in \{1, \dots, n_y\}: \quad \|h_i(\boldsymbol{x}(t)) - p_i(\theta(t))\| < \psi_{0,i}(t).$$

ii) ***Convergence on path****: The system moves along* $\mathcal{P}$ *such that*

$$\lim_{t\to\infty} \|\theta(t)\| = 0.$$

Here we consider an output path-following problem with *prescribed path accuracy*, i.e. we want to enforce that the absolute value of each path-following error $|h_i(\boldsymbol{x}) - p_i(\theta)|$ is always bounded by the prescribed function $\psi_{i,0}(\cdot)$. One should note that in the literature path-following problems usually require convergence of the output to the path (cf. [1], [7]) instead of *prescribed path accuracy*. Furthermore, the convergence-on-path requirement is sometimes replaced by strict forward motion, i.e. it can be required that $\dot{\theta}(t) > 0$ holds for all t, see [1].

The main idea of path-following is to regard the path parameter θ as a virtual state of the control problem whose dynamics are governed by a timing law, e.g. of the form $\dot{\theta} = g(\theta, v)$ where $g\colon \mathbb{R}\times\mathbb{R} \to \mathbb{R}_{>0}$ (see [1], [2]). The timing law includes an additional (virtual) control input v.[1] In the following we will use this extra input to control the evolution of the reference along $\mathcal{P}$ and to enforce prescribed path accuracy. However, we do not use a first-order timing law. For $\hat{r} \in \mathbb{N}$, we consider a chain of integrators as dynamics of θ, i.e.

$$\theta^{(\hat{r})}(t) = v(t), \qquad \theta^{(i)}(0) = \theta_0^{(i)},\ i \in \{1, \dots, \hat{r}\}. \tag{3}$$

The length of this chain of integrators is chosen to equal the maximum element of the vector relative degree of system (1a). Similar to [3], [7] we rely on this timing law and tackle path-following problems via an augmented system description

$$\dot{\boldsymbol{x}} = \boldsymbol{f}(\boldsymbol{x}) + \sum_{j=1}^{n_u} \boldsymbol{g}_j(\boldsymbol{x}) u_j, \quad \boldsymbol{x}(0) = \boldsymbol{x}_0 \in \mathbb{R}^{n_x} \tag{4a}$$

$$\dot{\boldsymbol{z}} = \widetilde{\boldsymbol{I}}_{\hat{r}} \boldsymbol{z} + \begin{pmatrix} \boldsymbol{0}_{\hat{r}-1} \\ 1 \end{pmatrix} v, \quad \boldsymbol{z}(0) = \boldsymbol{z}_0 \in \mathbb{R}^{\hat{r}} \tag{4b}$$

$$\boldsymbol{e} = \boldsymbol{h}(\boldsymbol{x}) - \boldsymbol{p}(z_1), \tag{4c}$$

$$\theta = z_1. \tag{4d}$$

Here, (4a) includes the dynamics of the system to be controlled (1a); in (4b) the timing law (3) is written with $\boldsymbol{z} = (\theta, \dot{\theta}, \dots, \theta^{(\hat{r}-1)})^\top$. The error output (4c) represents the deviation from the path and (4d) describes the current reference position on the path.

The main idea behind this augmented system description for path-following problems is that (4) can be mapped into path-following specific coordinates, i.e. a so-called *transverse normal form* [3], [5]. We will show later that this description of path-following problems allows the design of path-following funnel controllers for rigid-link revolute-joint robotic systems.

Rigid-link revolute-joint robotic systems

Subsequently, we restrict the investigations to path following for rigid, fully-actuated robotic systems with n exclusively revolute joints, $n \in \mathbb{N}$. Such a n degree-of-freedom robotic manipulator is described by

$$\begin{pmatrix} \dot{\boldsymbol{x}}_1 \\ \dot{\boldsymbol{x}}_2 \end{pmatrix} = \begin{pmatrix} \boldsymbol{x}_2 \\ \boldsymbol{M}(\boldsymbol{x}_1)^{-1}\big[-\boldsymbol{C}(\boldsymbol{x}_1, \boldsymbol{x}_2)\boldsymbol{x}_2 - \boldsymbol{g}(\boldsymbol{x}_1) - \boldsymbol{d}(t) + \boldsymbol{u}\big] \end{pmatrix} \tag{5a}$$

$$\boldsymbol{y} = (y_1, \dots, y_n)^\top = \boldsymbol{x}_1 \tag{5b}$$

with initial value $(\boldsymbol{x}_1(0), \boldsymbol{x}_2(0)) = (\boldsymbol{x}_1^0, \boldsymbol{x}_2^1) \in \mathbb{R}^{2n}$. For details on this model we refer to [13, p. 77]. The signals $\boldsymbol{x}_1$ in $[\mathrm{rad}]^n$ and $\boldsymbol{x}_2$ in $[\mathrm{rad/s}]^n$ represent joint angle and joint speed (vector), respectively. $\boldsymbol{M}(\cdot) \in \mathcal{C}(\mathbb{R}^n; \mathbb{R}^{n\times n})$ is the position dependent inertia matrix. For our approach, the inertia matrix $\boldsymbol{M}(\cdot)$ must be known. Matrix $\boldsymbol{C}(\cdot,\cdot) \in \mathcal{C}(\mathbb{R}^{2n}; \mathbb{R}^{n\times n})$ is the position and speed dependent centrifugal and Coriolis force matrix. $\boldsymbol{d}(\cdot) \in \mathcal{L}^\infty(\mathbb{R}_{\geq 0}; \mathbb{R}^n)$ represents an exogenous disturbance and $\boldsymbol{g}(\cdot) \in \mathcal{C}(\mathbb{R}^n; \mathbb{R}^n)$ is the position dependent gravity vector. The robot is actuated by joint torque vector $\boldsymbol{u}$ $[\mathrm{Nm}]^n$ (control input). We do not consider friction. The following assumptions are imposed on model (5) and path (2):

(A_1) the inertia matrix is uniformly bounded from above and below (see e.g. [14]), i.e. $\exists\, \overline{c}_{\boldsymbol{M}}, \underline{c}_{\boldsymbol{M}} > 0\ \forall\, \boldsymbol{y} \in \mathbb{R}^n$:

$$0 < \underline{c}_{\boldsymbol{M}} \boldsymbol{I}_n \leq \boldsymbol{M}(\boldsymbol{y}) = \boldsymbol{M}(\boldsymbol{y})^\top \leq \overline{c}_{\boldsymbol{M}} \boldsymbol{I}_n;$$

(A_2) the centrifugal and Coriolis force matrix is upper bounded (see e.g. [13, Sections 4.2]) as follows

$$\exists\, c_{\boldsymbol{C}} > 0\ \forall\, \boldsymbol{y}, \boldsymbol{v}, \boldsymbol{w} \in \mathbb{R}^n\colon\ \|\boldsymbol{C}(\boldsymbol{y}, \boldsymbol{v})\boldsymbol{w}\| \leq c_{\boldsymbol{C}} \|\boldsymbol{v}\| \|\boldsymbol{w}\|;$$

(A_3) the gravity vector is uniformly bounded (see e.g. [13, Sections 4.3]), i.e. $\exists\, c_{\boldsymbol{g}} > 0\ \forall\, \boldsymbol{y} \in \mathbb{R}^n\colon\ \|\boldsymbol{g}(\boldsymbol{y})\| \leq c_{\boldsymbol{g}}$;

[1] The problem of tracking output trajectories can be understood as a special case of output path-following with fixed reference timing, i.e. in $\dot{\theta} = g(\theta)$. The external input v does not appear.

(A_4) the exogenous disturbance is bounded, i.e. $\boldsymbol{d}(\cdot) \in \mathcal{L}^\infty(\mathbb{R}_{\geq 0}, \mathbb{R}^n)$

(A_5) joint angles $\boldsymbol{x}_1(\cdot)$ and velocities $\boldsymbol{x}_2(\cdot)$ are available for feedback (measured signals);

(A_6) the path $\mathcal{P}$ is contained in a compact subset $\tilde{\mathcal{P}} \subset \mathbb{R}^n$ and its parametrization satisfies $\boldsymbol{p}(\cdot) \in \mathcal{C}^2 \cap \mathcal{W}^{2,\infty}(\mathbb{R}; \mathbb{R}^n)$.

Assumptions (A_1)-(A_3) are intrinsic properties of rigid robotic manipulators with exclusively revolute joints (see e.g. [13, Sections 4.1-4.3]). Assumptions (A_4)-(A_5) are realistic for position control problems of mechatronic systems (see e.g. [10] and [15, p. 210-213 and 290-292]). Assumption (A_6) is used to simplify the proof of our main result in Sec. IV.

III. Funnel control for rigid-link revolute-joint robotic systems

Funnel control (see e.g. [8]–[11]) is a high-gain based time-varying output feedback control strategy which guarantees *tracking with prescribed transient accuracy*. It allows for gain increase *and* decrease (in contrast to classical high-gain adaptive controllers). Measurement noise is tolerated (but neglected in this paper). Simple root locus analysis show that relative-degree-two systems are not in general stabilizable by simple high-gain output feedback: either a backstepping controller [9] or derivative feedback [11] is necessary.

Based on the single-input single-output (SISO) results in [10], [11] of funnel control with derivative feedback for relative-degree-two systems and its application to position control problems of mechatronic systems, an extension to the multi-input multi-output (MIMO) case of rigid-link revolute-joint robots (5) with *known* inertia matrix is presented in [16].

For a given *time-varying* reference $\boldsymbol{y}_{\mathrm{ref}}(\cdot) := (y_{i,\mathrm{ref}}(\cdot), \dots, y_{n,\mathrm{ref}}(\cdot))^\top \in \mathcal{W}^{2,\infty}(\mathbb{R}_{\geq 0}; \mathbb{R}^n)$, the control objective is *tracking with prescribed transient accuracy* for position and speed tracking error of each joint $i \in \{1, \dots, n\}$ (see Fig. 1), i.e.

$$\begin{aligned} \forall\, t \geq 0\colon \quad & |e_i(t)| = |y_{i,\mathrm{ref}}(t) - y_i(t)| < \psi_{0,i}(t) \quad \wedge \\ & |\dot{e}_i(t)| = |\dot{y}_{i,\mathrm{ref}}(t) - \dot{y}_i(t)| < \psi_{1,i}(t) \end{aligned} \tag{6}$$

where $\boldsymbol{\psi}_0(\cdot) := (\psi_{0,1}(\cdot), \dots, \psi_{0,n}(\cdot))^\top \in \mathcal{W}^{1,\infty}(\mathbb{R}_{\geq 0}; (0,\infty))$ and $\boldsymbol{\psi}_1(\cdot) := (\psi_{1,1}(\cdot), \dots, \psi_{1,n}(\cdot))^\top \in \mathcal{W}^{1,\infty}(\mathbb{R}_{\geq 0}; (0,\infty))$ are the sub-funnel boundaries for position and speed error, respectively. For all $i \in \{1, \dots, n\}$, the boundary functions $(\psi_{0,i}(\cdot),\ \psi_{1,i}(\cdot))$ are chosen from

$$\mathcal{B}_2 := \left\{ (\psi_0, \psi_1)\colon \mathbb{R}_{\geq 0} \to \mathbb{R}^2 \;\middle|\; \begin{array}{l} \text{(i) } \forall\, i \in \{0,1\}\ \exists\, c_i > 0\colon \psi_i(\cdot) \in \mathcal{W}^{1,\infty}(\mathbb{R}_{\geq 0}, [c_i, \infty)) \\ \text{(ii) } \exists\, \delta > 0 \text{ for a.a. } t \geq 0\colon \psi_1(t) \geq -\frac{\mathrm{d}}{\mathrm{d}t}\psi_0(t) + \delta \end{array} \right\}. \tag{7}$$

Condition (ii) in (7) is essential: only if an error derivative with $\operatorname{sign}(e_i(t))\dot{e}_i(t) < \frac{\mathrm{d}}{\mathrm{d}t}\psi_{0,i}(t)$ is admissible/feasible, then the error $e_i(t)$ "may depart" from sub-boundary $\psi_{0,i}(t)$ (see Fig. 1). In other words, for funnel boundary $(\boldsymbol{\psi}_0(\cdot), \boldsymbol{\psi}_1(\cdot)) \in \mathcal{B}_2^n$ (with $\mathcal{B}_2$ as in (7)), tracking error

$$\boldsymbol{e}(\cdot) = \boldsymbol{y}(\cdot) - \boldsymbol{y}_{\mathrm{ref}}(\cdot) \tag{8}$$

and speed tracking error $\dot{\boldsymbol{e}}(\cdot) = \dot{\boldsymbol{y}}(\cdot) - \dot{\boldsymbol{y}}_{\mathrm{ref}}(\cdot)$ shall evolve within the "performance funnel" given by

$$\begin{aligned} \mathcal{F}_{(\boldsymbol{\psi}_0, \boldsymbol{\psi}_1)} := \big\{ & (t, \boldsymbol{\xi}, \boldsymbol{\eta}) \in \mathbb{R}_{\geq 0} \times \mathbb{R}^n \times \mathbb{R}^n \;\big| \\ & \forall\, i \in \{1, \dots, n\}\colon \ |\xi_i| < \psi_{0,\,i}(t) \wedge |\eta_i| < \psi_{1,\,i}(t) \big\}, \end{aligned} \tag{9}$$

i.e. $(t, \boldsymbol{e}(t), \dot{\boldsymbol{e}}(t)) \in \mathcal{F}_{(\boldsymbol{\psi}_0, \boldsymbol{\psi}_1)}$ for all $t \geq 0$. The asymptotic accuracies of the limiting functions (see Fig. 1) are given by

$$\lambda_{0,i} := \liminf_{t \to \infty} \psi_{0,i}(t) \qquad \text{and} \qquad \lambda_{1,i} := \liminf_{t \to \infty} \psi_{1,i}(t).$$

Example 1. *Let $\Lambda_{0,i} \geq \lambda_{0,i} > 0$, $T_E > 0$ [s] and $\lambda_{1,i} > 0$ [s] for $i \in \{1, \dots, n\}$, then a possible i-th sub-boundary is*

$$\begin{aligned} (\psi_{0,i},\, \psi_{1,i})\colon \mathbb{R}_{\geq 0} \to (\lambda_{0,i}, \Lambda_{0,i}] \times (\lambda_{1,i},\, (\Lambda_{0,i} - \lambda_{0,i})/T_E], \\ t \mapsto \begin{pmatrix} (\Lambda_{0,i} - \lambda_{0,i}) \exp\left(-t/T_E\right) + \lambda_{0,i} \\ \frac{\Lambda_{0,i} - \lambda_{0,i}}{T_E} \exp\left(-t/T_E\right) + \lambda_{1,i} \end{pmatrix}. \end{aligned} \tag{10}$$

Boundary (10) *is positive, non-increasing, bounded and smooth. Its asymptotic accuracies are given by $(\lambda_{0,i},\ \lambda_{1,i})$. The boundary 'starts' at $(\Lambda_{0,i},\ \frac{\Lambda_{0,i} - \lambda_{0,i}}{T_E} + \lambda_{1,i})$ and its derivative is essentially bounded by $\big((\Lambda_{0,i} - \lambda_{0,i})/T_E,\ (\Lambda_{0,i} - \lambda_{0,i})/T_E^2\big)$. By setting $\delta_i := \lambda_{1,i}$ and noting that $\psi_{1,i}(t) \geq -\dot{\psi}_{0,i}(t) + \delta_i$ for (almost) all $t \geq 0$ in* (10)*, it is easy to see that* (10) *is element of $\mathcal{B}_2$.*

If the inertia matrix $\boldsymbol{M}(\cdot)$ of (5) is known, then the MIMO funnel controller is a simple proportional-derivative controller. Its properties are stated in the following theorem, see also Theorem 3.1 in [16].

Theorem 1.
Let $n \in \mathbb{N}$ and consider a n-th DOF rigid-link revolute-joint robotic manipulator of form (5) *with known inertia matrix $\boldsymbol{M}(\cdot)$ and which satisfies assumptions (A_1)-(A_5). Then, for arbitrary position reference $\boldsymbol{y}_{\mathrm{ref}}(\cdot) \in \mathcal{W}^{2,\infty}(\mathbb{R}_{\geq 0}, \mathbb{R}^n)$, funnel boundary $(\boldsymbol{\psi}_0(\cdot), \boldsymbol{\psi}_1(\cdot)) \in \mathcal{B}_2^n$, gain scaling $\boldsymbol{\varsigma}_0(\cdot),\ \boldsymbol{\varsigma}_1(\cdot) \in \mathcal{W}^{1,\infty}(\mathbb{R}_{\geq 0}; [c, \infty)^n)$, $c > 0$ and initial value $(\boldsymbol{x}_1^0, \boldsymbol{x}_2^1) \in \mathbb{R}^{2n}$ satisfying $\forall\, i \in \{1, \dots, n\}$:*

$$|x_{1,i}^0 - y_{\mathrm{ref,i}}(0)| < \psi_{0,i}(0) \ \text{ and } \ |x_{2,i}^1 - \dot{y}_{\mathrm{ref,i}}(0)| < \psi_{1,i}(0), \tag{11}$$

the MIMO funnel controller

$$\boldsymbol{u}(t) = -\boldsymbol{M}(\boldsymbol{x}_1(t)) \Big(\boldsymbol{K}_0(t)^2 \boldsymbol{e}(t) + \boldsymbol{K}_0(t) \boldsymbol{K}_1(t) \dot{\boldsymbol{e}}(t) \Big) \tag{12}$$

with gain matrices

$$\left. \begin{aligned} & \boldsymbol{K}_0(t) = \begin{bmatrix} k_{0,1}(t) & & \\ & \ddots & \\ & & k_{0,n}(t) \end{bmatrix},\ k_{0,i}(t) = \frac{\varsigma_{0,i}(t)}{\psi_{0,i}(t) - |e_i(t)|} \\ & \text{and} \\ & \boldsymbol{K}_1(t) = \begin{bmatrix} k_{1,1}(t) & & \\ & \ddots & \\ & & k_{1,n}(t) \end{bmatrix},\ k_{1,i}(t) = \frac{\varsigma_{1,i}(t)}{\psi_{1,i}(t) - |\dot{e}_i(t)|}, \\ & \text{where } i \in \{1, \dots, n\}, \end{aligned} \right\} \tag{13}$$

applied to (5) *yields a closed-loop initial-value problem with the properties:*

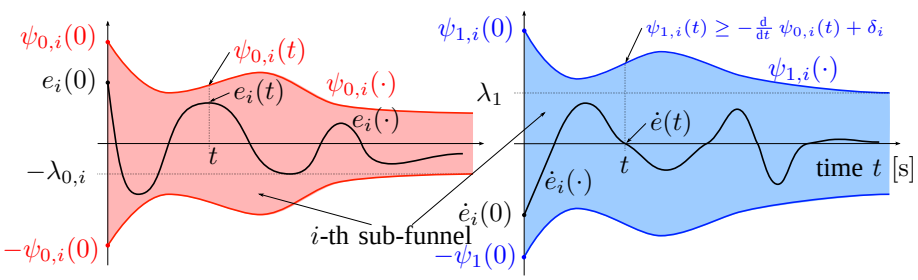

Fig. 1: *i-th sub-funnel for the i-th joint, $i \in \{1, \dots, n\}$: Position error $e_i(\cdot)$ and speed error $\dot{e}_i(\cdot)$ with sub-funnel boundaries $\psi_{0,i}(\cdot)$ and $\psi_{1,i}(\cdot)$.*

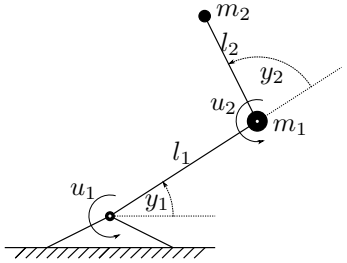

Fig. 2: *Planar (elbow-like) rigid-link revolute-joint robotic manipulator.*

(i) there exists a solution[2] $(\boldsymbol{x}_1(\cdot), \boldsymbol{x}_2(\cdot)) : [0, T) \to \mathbb{R}^{2n}$ *which can be maximally extended and* $T \in (0, \infty]$*;*

(ii) the solution $(\boldsymbol{x}_1(\cdot), \boldsymbol{x}_2(\cdot))$ *does not have finite escape time, i.e.* $T = \infty$*;*

(iii) the tracking error $\boldsymbol{e}(\cdot)$ *as in* (8) *and* $\dot{\boldsymbol{e}}(\cdot)$ *are uniformly bounded away from the boundary, i.e.* $\forall\, i \in \{1, \dots, n\}\ \exists \varepsilon_{0,i}, \varepsilon_{1,i} > 0\ \forall\, t \geq 0 : \psi_{0,i}(t) - |e_i(t)| \geq \varepsilon_{0,i}$ *and* $\psi_{1,i}(t) - |\dot{e}_i(t)| \geq \varepsilon_{1,i}$*;*

(iv) control action and gains are bounded, i.e. $\boldsymbol{u}(\cdot) \in \mathcal{L}^\infty(\mathbb{R}_{\geq 0}; \mathbb{R}^n)$ *and* $\boldsymbol{K}_0(\cdot), \boldsymbol{K}_1(\cdot) \in \mathcal{L}^\infty(\mathbb{R}_{\geq 0}; \mathbb{R}^{n \times n})$.

Proof. See [16]. □

Remark 1 (Time-varying gains)**.** *Gain "adaptation" in* (12) *is—for each joint* $i \in \{1, \dots, n\}$*—as follows: Gain* $k_{0,i}(\cdot)$ *(or* $k_{1,i}(\cdot)$*) increases, if error* $e_i(\cdot)$ *(or* $\dot{e}_i(\cdot)$*) draws close to* $\psi_{0,i}(\cdot)$ *(or* $\psi_{1,i}(\cdot)$*) (more aggressive control) and decreases, if error* $e_i(\cdot)$ *(or* $\dot{e}_i(\cdot)$*) becomes small (more relaxed control).*

IV. Path-following funnel control

In this section we investigate the combination of funnel control and path-following. We will design a combined controller and, with that, will solve Problem 1 for rigid-link revolute-joint robots as in (5). The proposed design is based on a version of augmented system (4) that is tailored to form (5).

Clearly, the rigid-link revolute-joint robot in (5) has a global vector relative degree of $\boldsymbol{r} = (2, \dots, 2)^\top$.[3] Hence $\hat{r} = 2$ and we choose an integrator chain of length two as timing law (3). So the augmented system (4) for path-following of (5) reads

$$\begin{pmatrix} \dot{\boldsymbol{x}}_1 \\ \dot{\boldsymbol{x}}_2 \end{pmatrix} = \begin{pmatrix} \boldsymbol{x}_2 \\ \boldsymbol{M}(\boldsymbol{x}_1)^{-1}\big[-\boldsymbol{C}(\boldsymbol{x}_1, \boldsymbol{x}_2)\boldsymbol{x}_2 - \boldsymbol{g}(\boldsymbol{x}_1) - \boldsymbol{d}(t) + \boldsymbol{u}\big] \end{pmatrix} \tag{14a}$$

$$\dot{\boldsymbol{z}} = \begin{bmatrix} 0 & 1 \\ 0 & 0 \end{bmatrix} \boldsymbol{z} + \begin{pmatrix} 0 \\ 1 \end{pmatrix} v, \tag{14b}$$

$$\boldsymbol{e} = \boldsymbol{x}_1 - \boldsymbol{p}(z_1) \tag{14c}$$

$$\theta = z_1 \tag{14d}$$

The initial conditions are $(\boldsymbol{x}_1(0), \boldsymbol{x}_2(0)) = (\boldsymbol{x}_1^0, \boldsymbol{x}_2^1) \in \mathbb{R}^{2n}$ and $\boldsymbol{z}(0) = \boldsymbol{z}^0 \in \mathbb{R}^2$.

[2] Solutions of ordinary differential equations are considered in the sense of Carathéodory (see e.g. Section 2.1.2 in [17]).

[3] Readers not familiar with the notion of a vector relative degree of a nonlinear system are referred to [18, Sec. 5.1].

We design the path-following funnel controller based on the augmented system description (14) including robot dynamics (14a) with control input $\boldsymbol{u}$ *and* the timing law (14b) with virtual input v. The combined controller will consist of two parts: the funnel controller as in (12) with its gains as in (13) and a (virtual) error-dependent feedback for the path timing given by

$$v(t) = -\boldsymbol{\kappa}\big(\boldsymbol{e}(t), \dot{\boldsymbol{e}}(t)\big)^\top \boldsymbol{z}(t) \tag{15}$$

where $\boldsymbol{\kappa} : \mathbb{R}^n \times \mathbb{R}^n \to \mathbb{R}^2$. Now, the interesting question is how to design the feedback for the virtual input v of (14b)? In principle, there are two options: either one relies on $v = -\boldsymbol{\kappa}^\top \boldsymbol{z}$, with $\boldsymbol{\kappa} \in \mathbb{R}^2_{>0}$ being constant, or one allows error-dependent path-parameter feedbacks of the form (15).

In the former case with $v = -\boldsymbol{\kappa}^\top \boldsymbol{z}$, it is straightforward to design $\boldsymbol{\kappa} \in \mathbb{R}^2_{>0}$ such that the timing dynamics (14b) are asymptotically stable. *However*, the degree of freedom to adjust the timing along the path with respect to current error information would be lost. This way one would turn the path-following problem into a tracking problem with $\boldsymbol{y}_{\mathrm{ref}}(\cdot) = \boldsymbol{p}(\theta(\cdot))$ and one could directly invoke Theorem 1 to conclude that path-following funnel control is feasible.

The latter case with v from (15) is more interesting. It has the appealing property that the current path deviation can influence the evolution of the reference $\boldsymbol{p}(z_1(\cdot))$. This way, one may e.g. slow down the path evolution $\boldsymbol{p}(z_1(\cdot))$ for large errors $\boldsymbol{e}(\cdot)$ and/or $\dot{\boldsymbol{e}}(\cdot)$. For this case, it is not yet clear how to design the gain $\boldsymbol{\kappa} : \mathbb{R}^n \times \mathbb{R}^n \to \mathbb{R}^2$ such that asymptotic stability is guaranteed. In the next theorem we present sufficient conditions guaranteeing stability of (14) subject to error-dependent timing (15) and funnel controller (12).

Theorem 2 (Path-following funnel control)**.**
Consider the augmented system (14) *and let assumptions* (A_1)*-*(A_6) *be satisfied. Moreover, assume the following holds*

(A$_7$) $\boldsymbol{\kappa}(\cdot,\cdot) := \big(\kappa_1(\cdot,\cdot), \kappa_2(\cdot,\cdot)\big)^\top \in \mathcal{C}^1(\mathbb{R}^n \times \mathbb{R}^n; \mathbb{R}^2)$ *in* (15) *and there exist real constants* $0 < \underline{\kappa} \leq \overline{\kappa}$ *such that for all* $\boldsymbol{\alpha}, \boldsymbol{\beta} \in \mathbb{R}^n$*:*

$$\left.\begin{array}{l} 0 < \underline{\kappa} \leq \kappa_1(\boldsymbol{\alpha}, \boldsymbol{\beta}) \leq \kappa_2(\boldsymbol{\alpha}, \boldsymbol{\beta}) \leq \overline{\kappa} \\ \text{and} \quad 1 + \underline{\kappa} \leq \kappa_2(\boldsymbol{\alpha}, \boldsymbol{\beta}). \end{array}\right\} \tag{16}$$

Then, for any funnel boundary $(\boldsymbol{\psi}_0(\cdot), \boldsymbol{\psi}_1(\cdot)) \in \mathcal{B}_2^n$*, gain scaling* $\boldsymbol{\varsigma}_0(\cdot), \boldsymbol{\varsigma}_1(\cdot) \in \mathcal{W}^{1,\infty}(\mathbb{R}_{\geq 0}; [c, \infty)^n)$*,* $c > 0$ *and initial value* $(\boldsymbol{x}_1^0, \boldsymbol{x}_2^1, \boldsymbol{z}^0) \in \mathbb{R}^n \times \mathbb{R}^n \times \mathbb{R}^2$ *satisfying* $\forall\, i \in$

$\{1,\dots,n\}$:

$$\left|x^0_{1,i} - p_i(z^0_1)\right| < \psi_{0,i}(0) \wedge \left|x^1_{2,i} - \frac{\partial p_i(z^0_1)}{\partial\theta}\, z^0_2\right| < \psi_{1,i}(0), \tag{17}$$

the MIMO path-following funnel controller (12) *with* (13) and *timing feedback* (15) *applied to* (14) *yields a closed-loop initial-value problem with the properties:*

- *(i) there exists a solution* $(\boldsymbol{x}_1,\, \boldsymbol{x}_2,\, \boldsymbol{z}) : [0,T) \to \mathbb{R}^n \times \mathbb{R}^n \times \mathbb{R}^2$ *which can be maximally extended and* $T \in (0,\infty]$*;*
- *(ii) the solution* $(\boldsymbol{x}_1,\, \boldsymbol{x}_2,\, \boldsymbol{z})$ *does not have finite escape time, i.e.* $T = \infty$*;*
- *(iii) the path error* $\boldsymbol{e}(\cdot)$ *as in* (14c) *and* $\dot{\boldsymbol{e}}(\cdot)$ *are uniformly bounded away from the boundary, i.e.* $\forall\, i \in \{1,\dots,n\}\ \exists \varepsilon_{0,i}, \varepsilon_{1,i} > 0\ \forall\, t \geq 0 : \psi_{0,\,i}(t) - |e_i(t)| \geq \varepsilon_{0,\,i}$ *and* $\psi_{1,i}(t) - |\dot{e}_i(t)| \geq \varepsilon_{1,i}$*;*
- *(iv) the timing dynamics* $\boldsymbol{z}(\cdot)$ *are asymptotically stable;*
- *(v) control action and gains are bounded, i.e.* $\boldsymbol{u}(\cdot) \in \mathcal{L}^\infty(\mathbb{R}_{\geq 0};\mathbb{R}^n)$, $v(\cdot) \in \mathcal{L}^\infty(\mathbb{R}_{\geq 0};\mathbb{R})$ *and* $\boldsymbol{K}_0(\cdot),\, \boldsymbol{K}_1(\cdot) \in \mathcal{L}^\infty(\mathbb{R}_{\geq 0};\mathbb{R}^{n\times n})$.

The main difficulty in proving Theorem 2 is due to the potential singularity in the right-hand side of the closed-loop system (14), (12), (15). Hence, existence of a global solution cannot be concluded by standard arguments and some care must be exercised. The proof is quite similar to the proof of Theorem 1 which can be found in [16]. And furthermore, we rely on the proof of Theorem 3.3 in [10]. Due to space limitations only the crucial steps are presented in detail.

Proof. Step 1: Some preliminaries
It is easy to see that (A_1) implies

$$\underline{\gamma_0}\boldsymbol{I}_n \leq \boldsymbol{\Gamma}_0(\boldsymbol{y}) := \boldsymbol{M}^{-1}(\boldsymbol{y}) = \boldsymbol{\Gamma}_0(\boldsymbol{y})^\top \leq \overline{\gamma_0}\boldsymbol{I}_n. \tag{18}$$

Define the constants $\forall\, i \in \{1,\dots,n\}$:

$$\begin{aligned} \underline{\varsigma}_{0,i} &:= \inf_{t\geq 0} \varsigma_{0,i}(t) \quad \text{and} \quad \underline{\varsigma}_{1,i} := \inf_{t\geq 0} \varsigma_{1,i}(t), \\ \lambda_{0,i} &:= \inf_{t\geq 0} \psi_{0,i}(t) \quad \text{and} \quad \lambda_{1,i} := \inf_{t\geq 0} \psi_{1,i}(t). \end{aligned} \tag{19}$$

Furthermore, for path error $\boldsymbol{e}$ as in (14c) the augmented system (14) may be written in the following form

$$\frac{\mathrm{d}}{\mathrm{d}t}\begin{pmatrix}\boldsymbol{e}\\ \dot{\boldsymbol{e}}\end{pmatrix} = \begin{pmatrix}\dot{\boldsymbol{e}}\\ \tilde{\boldsymbol{f}}(t,\boldsymbol{e},\dot{\boldsymbol{e}},\boldsymbol{z},\boldsymbol{u},v)\end{pmatrix},\ \begin{pmatrix}\boldsymbol{e}(0)\\ \dot{\boldsymbol{e}}(0)\end{pmatrix} = \begin{pmatrix}\boldsymbol{x}^0_1 - \boldsymbol{p}(z^0_1)\\ \boldsymbol{x}^1_2 - \dot{\boldsymbol{p}}(\boldsymbol{z}^0)\end{pmatrix} \tag{20a}$$

$$\dot{\boldsymbol{z}} = \begin{pmatrix}0 & 1\\ 0 & 0\end{pmatrix}\boldsymbol{z} + \begin{pmatrix}0\\ 1\end{pmatrix} v,\ \boldsymbol{z}(0) = \boldsymbol{z}^0 \tag{20b}$$

$$\theta = z_1 \tag{20c}$$

where $\dot{\boldsymbol{p}}(\boldsymbol{z}^0) := \dfrac{\partial \boldsymbol{p}(z^0_1)}{\partial\theta}\, z^0_2$ in (20a) and $\tilde{\boldsymbol{f}} : \mathbb{R}_{\geq 0}\times\mathbb{R}^n\times\mathbb{R}^n\times\mathbb{R}^2\times\mathbb{R}^n\times\mathbb{R}\to\mathbb{R}^{2n}\times\mathbb{R}^2$ reads

$$\begin{aligned} &\tilde{\boldsymbol{f}}(t,\boldsymbol{e},\dot{\boldsymbol{e}},\boldsymbol{z},\boldsymbol{u},v) = \boldsymbol{M}(\boldsymbol{e}+\boldsymbol{p}(z_1))^{-1}\cdot \\ &\Big[-\boldsymbol{C}\big(\boldsymbol{e}+\boldsymbol{p}(z_1),\dot{\boldsymbol{e}}+\frac{\partial\boldsymbol{p}(z_1)}{\partial\theta}\, z_2\big)\cdot\big(\dot{\boldsymbol{e}}+\frac{\partial\boldsymbol{p}(z_1)}{\partial\theta}\, z_2\big) \\ &-\boldsymbol{g}(\boldsymbol{e}+\boldsymbol{p}(z_1)) - \boldsymbol{d}(t) + \boldsymbol{u}\Big] - \frac{\partial^2\boldsymbol{p}(z_1)}{\partial\theta^2}\,(z_2)^2 - \frac{\partial\boldsymbol{p}(z_1)}{\partial\theta}\, v. \end{aligned}$$

Step 2: It is shown that Assertion (i) holds true, i.e. existence of a maximally extended solution.
It suffices to consider system (14) in the form (20). For $\mathcal{F}_{(\boldsymbol{\psi}_0,\boldsymbol{\psi}_1)}$ as in (9) define the non-empty and open set

$$\mathcal{D} := \Big\{(t,(\boldsymbol{\mu},\boldsymbol{\xi}),\boldsymbol{z}) \in \mathbb{R}_{\geq 0}\times\mathbb{R}^{2n}\times\mathbb{R}^2 \;\Big|\; (t,\boldsymbol{\mu},\boldsymbol{\xi}) \in \mathcal{F}_{(\boldsymbol{\psi}_0,\boldsymbol{\psi}_1)}\Big\}, \tag{21}$$

and the function $\boldsymbol{f}_{\mathrm{all}} : \mathcal{D}\to\mathbb{R}^n\times\mathbb{R}^n\times\mathbb{R}^2$, $(t,(\boldsymbol{\mu},\boldsymbol{\xi}),\boldsymbol{z})\mapsto$

$$\begin{pmatrix} \boldsymbol{\xi} \\ \boldsymbol{\Gamma}_0(\boldsymbol{\mu}+\boldsymbol{p}(z_1))\Big[-\boldsymbol{C}\Big(\boldsymbol{\mu}+\boldsymbol{p}(z_1),\,\boldsymbol{\xi}+\frac{\partial\boldsymbol{p}(z_1)}{\partial\theta}\, z_2\Big)\cdot \\ \cdot\Big(\boldsymbol{\xi}+\frac{\partial\boldsymbol{p}(z_1)}{\partial\theta}\, z_2\Big) - \boldsymbol{g}(\boldsymbol{\mu}+\boldsymbol{p}(z_1)) - \boldsymbol{d}(t)\Big] - \frac{\partial^2\boldsymbol{p}(z_1)}{\partial\theta^2}\, z_2^2 \\ -\frac{\partial\boldsymbol{p}(z_1)}{\partial\theta}\,\boldsymbol{\kappa}(\boldsymbol{e},\dot{\boldsymbol{e}})^\top\boldsymbol{z} - \operatorname{diag}\Big\{\frac{\varsigma_{0,1}(t)}{\psi_{0,1}(t)-|\mu_1|},\dots,\frac{\varsigma_{0,n}(t)}{\psi_{0,n}(t)-|\mu_n|}\Big\}^2\boldsymbol{\mu} \\ -\operatorname{diag}\Big\{\frac{\varsigma_{0,1}(t)\varsigma_{1,1}(t)}{(\psi_{0,1}(t)-|\mu_1|)(\psi_{1,1}(t)-|\xi_1|)},\dots, \\ \frac{\varsigma_{0,n}(t)\varsigma_{1,n}(t)}{(\psi_{0,n}(t)-|\mu_n|)(\psi_{1,n}(t)-|\xi_n|)}\Big\}\boldsymbol{\xi} \\ \begin{pmatrix}0 & 1\\ -\kappa_1(\boldsymbol{e},\dot{\boldsymbol{e}}) & -\kappa_2(\boldsymbol{e},\dot{\boldsymbol{e}})\end{pmatrix}\boldsymbol{z} \end{pmatrix}.$$

Then, for state variable $\widehat{\boldsymbol{x}} := (\boldsymbol{e},\dot{\boldsymbol{e}},\boldsymbol{z})$, the initial-value problem (12), (15),(20) may be expressed in standard form

$$\frac{\mathrm{d}}{\mathrm{d}t}\,\widehat{\boldsymbol{x}}(t) = \boldsymbol{f}_{\mathrm{all}}(t,\widehat{\boldsymbol{x}}(t)),\ \ \widehat{\boldsymbol{x}}(0) = \begin{pmatrix}\boldsymbol{x}^0_1 - \boldsymbol{p}(z^0_1)\\ \boldsymbol{x}^1_2 - \dot{\boldsymbol{p}}(\boldsymbol{z}^0)\\ \boldsymbol{z}^0\end{pmatrix}. \tag{22}$$

Furthermore, for any compact set $\mathcal{T}\times\mathcal{S}\subset\mathcal{D}$ there exist constants $m_{\mathcal{S}}, M_{\mathcal{S}}, P_{\mathcal{S}}, Q_{\mathcal{S}} > 0$ such that for all $(t,(\boldsymbol{\mu},\boldsymbol{\xi},\boldsymbol{z}))\in\mathcal{T}\times\mathcal{S}$:

$$\|(t,(\boldsymbol{\mu},\boldsymbol{\xi},\boldsymbol{z}))\| \leq M_{\mathcal{S}} \tag{23a}$$

$$\min_{i\in\{1,\dots,n\}}\{\psi_{0,i}(t)-|\mu_i|,\ \psi_{1,i}(t)-|\xi_i|\} \geq m_{\mathcal{S}} \tag{23b}$$

$$\left\|\frac{\partial\boldsymbol{p}(z_1)}{\partial\theta}\, z_2\right\| \leq P_{\mathcal{S}} \tag{23c}$$

$$\left\|\frac{\partial^2\boldsymbol{p}(z_1)}{\partial\theta^2}\, z_2^2\right\| \leq Q_{\mathcal{S}} \wedge \left\|\frac{\partial\boldsymbol{p}(z_1)}{\partial\theta}\,\boldsymbol{\kappa}(\boldsymbol{e},\dot{\boldsymbol{e}})^\top\boldsymbol{z}\right\| \leq Q_{\mathcal{S}}. \tag{23d}$$

Then, for $\boldsymbol{d}(\cdot)\in\mathcal{L}^\infty(\mathbb{R}_{\geq 0};\mathbb{R}^n)$ and $\boldsymbol{\varsigma}_0(\cdot),\boldsymbol{\varsigma}_1(\cdot)\in\mathcal{W}^{1,\infty}(\mathbb{R}_{\geq 0},\mathbb{R}^n_{>0})$, and in view of Assumptions (A_1)-(A_7), the function $\boldsymbol{f}_{\mathrm{all}}(\cdot,\cdot)$ has the following properties:

(i) $\boldsymbol{f}_{\mathrm{all}}(t,\cdot)$ is continuous for each fixed $t\geq 0$;
(ii) for each fixed $(\boldsymbol{\mu},\boldsymbol{\xi},\boldsymbol{z})\in\mathcal{S}$ the function $\boldsymbol{f}_{\mathrm{all}}(\cdot,(\boldsymbol{\mu},\boldsymbol{\xi},\boldsymbol{z}))$ is measurable;
(iii) for almost all $t\geq 0$ and for all $(\boldsymbol{\mu},\boldsymbol{\xi},\boldsymbol{z})\in\mathcal{S}$ we have

$$\begin{aligned} \|\boldsymbol{f}_{\mathrm{all}}(t,(\boldsymbol{\mu},\boldsymbol{\xi},\boldsymbol{z}))\| &\overset{(A_1)-(A_7),\ (23)}{\leq} M_{\mathcal{S}} \\ &+\overline{\gamma_0}\Big[c_{\boldsymbol{C}}(P_{\mathcal{S}}+M_{\mathcal{S}})^2 + M_{\mathcal{S}} + c_{\boldsymbol{g}} + \|\boldsymbol{d}(t)\|\Big] + 2Q_{\mathcal{S}} \\ &+\|\boldsymbol{\varsigma}_0(t)\|\,\big(\,\|\boldsymbol{\varsigma}_0(t)\| + \|\boldsymbol{\varsigma}_1(t)\|\,\big)M_{\mathcal{S}}/m^2_{\mathcal{S}} \\ &+(2\overline{\kappa}^2+1)M_{\mathcal{S}} =: l_{\mathcal{S}}(t) \end{aligned}$$

where $l_{\mathcal{S}}(\cdot)\in\mathcal{L}^\infty(\mathbb{R}_{\geq 0};\mathbb{R}_{\geq 0})\subset\mathcal{L}^1_{\mathrm{loc}}(\mathbb{R}_{\geq 0},\mathbb{R}_{\geq 0})$; and
(iv) for any compact set $\mathfrak{C}\subset\mathcal{T}\times\mathcal{S}$ there exists a function $\widetilde{l}_{\mathfrak{C}}(\cdot)\in\mathcal{L}^1(\mathbb{R};\mathbb{R}_{\geq 0})$ such that for all $(t,\widetilde{\boldsymbol{x}})$, $(t,\widetilde{\boldsymbol{y}})\in\mathfrak{C}$:

$$\|\boldsymbol{f}_{\mathrm{all}}(t,\widetilde{\boldsymbol{x}}) - \boldsymbol{f}_{\mathrm{all}}(t,\widetilde{\boldsymbol{y}})\| \leq \widetilde{l}_{\mathfrak{C}}(t)\,\|\widetilde{\boldsymbol{x}}-\widetilde{\boldsymbol{y}}\|.$$

Hence $\boldsymbol{f}_{\mathrm{all}}(\cdot,\cdot)$ is a Carathéodory function (see [17, p. 84]) and invoking Theorem 2.1.14 in [17] yields existence of

a solution $\widehat{\boldsymbol{x}} : [0,T) \to \mathbb{R}^{2n} \times \mathbb{R}^2$ of the initial-value problem (22) with $\widehat{\boldsymbol{x}}([0,T)) \in \mathcal{D}$, $T \in (0,\infty]$. Each solution can be extended to a maximal solution. Moreover $\boldsymbol{f}_{\text{all}}(\cdot,\cdot)$ is essentially bounded and so, if $T < \infty$, then for any compact $\mathfrak{C} \subset \mathcal{D}$, there exists $\tilde{t} \in [0,T)$ such that $\widehat{\boldsymbol{x}}(\tilde{t}) \notin \mathfrak{C}$. In the following, let $\widehat{\boldsymbol{x}} := (\boldsymbol{e}, \dot{\boldsymbol{e}}, \boldsymbol{z})\colon [0,T) \to \mathbb{R}^n \times \mathbb{R}^n \times \mathbb{R}^2$ be a fixed and maximally extended solution of the initial-value problem (22). Note that $(\boldsymbol{e}, \dot{\boldsymbol{e}}, \boldsymbol{z}) : [0,T) \to \mathbb{R}^n \times \mathbb{R}^n \times \mathbb{R}^2$ solves the closed-loop initial-value problem (20), (12), (15) for almost all $t \in [0,T)$. This shows Assertion (i).

Step 3: Some technical inequalities are introduced.
In view of Step 1, $\boldsymbol{e}(\cdot)$ and $\dot{\boldsymbol{e}}(\cdot)$ are continuous on $[0,T)$ and evolve within the funnel $\mathcal{F}_{(\boldsymbol{\psi}_0, \boldsymbol{\psi}_1)}$ as in (9). Moreover, due to the properties of $\mathcal{B}_2$ in (7), it follows that $\forall\, i \in \{1,\dots,n\}\ \forall\, t \in [0,T) : |e_i(t)| < \psi_{0,i}(t) \leq \|\psi_{0,i}\|_\infty$ and $|\dot{e}_i(t)| < \psi_{1,i}(t) \leq \|\psi_{1,i}\|_\infty$. Hence

$$\forall\, t \in [0,T) : \ \|\boldsymbol{e}(t)\| < \|\boldsymbol{\psi}_0\|_\infty \wedge \|\dot{\boldsymbol{e}}(t)\| < \|\boldsymbol{\psi}_1\|_\infty. \quad (24)$$

In view of (A_7) and Theorem 2.14 in [19], the timing closed-loop sub-system (14b), (15) is uniformly stable and its solution evolves within a forward invariant compact set. Hence,

$$\exists M_{\boldsymbol{z}} > 0\ \forall\, t \in [0,T) : \ \|\boldsymbol{z}(t)\| \leq M_{\boldsymbol{z}}. \quad (25)$$

Now, define $\widehat{\boldsymbol{d}}\colon\ \mathbb{R}_{\geq 0} \times \mathbb{R}^n \times \mathbb{R}^n \times \mathbb{R}^2 \to \mathbb{R}^n$

$$(t, \boldsymbol{\mu}, \boldsymbol{\xi}, \boldsymbol{z}) \mapsto \widehat{\boldsymbol{d}}(t, \boldsymbol{\mu}, \boldsymbol{\xi}, \boldsymbol{z}) := \boldsymbol{\Gamma}_0(\boldsymbol{\mu} + \boldsymbol{p}(z_1)) \cdot \Bigg[-\boldsymbol{C}\left(\boldsymbol{\mu} + \boldsymbol{p}(z_1),\, \boldsymbol{\xi} + \frac{\partial \boldsymbol{p}(z_1)}{\partial \theta}\, z_2\right)\left(\boldsymbol{\xi} + \frac{\partial \boldsymbol{p}(z_1)}{\partial \theta}\, z_2\right) - \boldsymbol{g}(\boldsymbol{\mu} + \boldsymbol{p}(z_1)) - \boldsymbol{d}(t)\Bigg] - \frac{\partial^2 \boldsymbol{p}(z_1)}{\partial \theta^2}\, z_2^2 - \frac{\partial \boldsymbol{p}(z_1)}{\partial \theta}\, \boldsymbol{\kappa}(\boldsymbol{\mu}, \boldsymbol{\xi})^\top \boldsymbol{z}$$

and the constant

$$M := \overline{\gamma_0}\left[c_{\boldsymbol{C}} \left(\| \frac{\partial \boldsymbol{p}}{\partial \theta} \|_\infty M_z + \|\boldsymbol{\psi}_1\|_\infty \right)^2 + c_{\boldsymbol{g}} + \|\boldsymbol{d}\|_\infty \right] + \| \frac{\partial^2 \boldsymbol{p}}{\partial \theta^2} \|_\infty M_{\boldsymbol{z}}^2 + \| \frac{\partial \boldsymbol{p}}{\partial \theta} \|_\infty \sqrt{2\overline{\kappa}}\, M_{\boldsymbol{z}}. \quad (26)$$

Invoking Assumptions (A_1)–(A_7) yields

$$\text{for a.a. } t \in [0,T): \ \left\| \widehat{\boldsymbol{d}}\big(t, \boldsymbol{e}(t), \dot{\boldsymbol{e}}(t), \boldsymbol{z}(t)\big) \right\| \overset{(18)}{\leq} \boldsymbol{\Gamma}_0(\boldsymbol{e}(t) + \boldsymbol{p}(z_1(t))) \Bigg[-\boldsymbol{C}(\cdot) \cdot \left(\dot{\boldsymbol{e}}(t) + \frac{\partial \boldsymbol{p}(z_1(t))}{\partial \theta}\, z_2(t) \right) - \boldsymbol{g}(\boldsymbol{e}(t) + \boldsymbol{p}(z_1(t))) - \boldsymbol{d}(t) \Bigg] - \frac{\partial^2 \boldsymbol{p}(z_1(t))}{\partial \theta^2}\, z_2(t)^2 - \frac{\partial \boldsymbol{p}(z_1(t))}{\partial \theta}\, \boldsymbol{\kappa}(\boldsymbol{e}(t), \dot{\boldsymbol{e}}(t))^\top \boldsymbol{z}(t) \overset{(24),(26)}{\leq} M,$$

It follows from Assumptions (A_1)–(A_7) that $\forall\, i \in \{1,\dots,n\}$ for a.a. $t \in [0,T)$:

$$|\widehat{d}_i\big(t, \boldsymbol{e}(t), \dot{\boldsymbol{e}}(t), \boldsymbol{z}(t)\big)| \leq M. \quad (27)$$

Inserting (12) and (15) into (20a) and invoking (27) yields

$$\forall\, i \in \{1,\dots,n\}\ \forall\, t \in [0,T) : \\ -M - k_{0,i}(t)^2\, e_i(t) - k_{0,i}(t)\, k_{1,i}(t)\, \dot{e}_i(t) \leq \ddot{e}_i(t) \\ \leq M - k_{0,i}(t)^2\, e_i(t) - k_{0,i}(t)\, k_{1,i}(t)\, \dot{e}_i(t). \quad (28)$$

Step 4: For all $i \in \{1,\dots,n\}$ it is shown that $|e_i(\cdot)|$ is uniformly bounded away from the boundary $\psi_{0,i}(\cdot)$; more precisely for positive

$$\varepsilon_{0,i} \ \leq\ \min\Big\{ \tfrac{\lambda_{0,i}}{4},\, \tfrac{\psi_{0,i}(0) - |e_i(0)|}{2},\, \tfrac{\frac{1}{2}\delta_i \varsigma_{0,i}^2 \lambda_{0,i}}{\beta + \sqrt{\beta^2 + 2\delta_i^2 \varsigma_{0,i}^2 \lambda_{0,i} M}},\, \tfrac{\frac{1}{2}\delta_i \varsigma_{0,i} \lambda_{0,i}}{2\|\varsigma_{1,i}\|_\infty \|\psi_{1,i}\|_\infty + \sqrt{4\|\varsigma_{1,i}\|_\infty^2 \|\psi_{1,i}\|_\infty^2 + 2\delta_i^2 \lambda_{0,i}(M + \|\dot{\psi}_{1,i}\|_\infty)}} \Big\}, \quad (29)$$

with $\beta := 2\varsigma_{0,i}\|\varsigma_{1,i}\|_\infty \|\psi_{1,i}\|_\infty + \delta_i \left(\|\psi_{1,i}\|_\infty + \|\dot{\psi}_{0,i}\|_\infty \right)^2$, $\lambda_{0,i}$, $\lambda_{1,i}$, $\varsigma_{0,i}$ *and* $\varsigma_{1,i}$ *as in* (19), $\delta_i = \delta$ *as in* (7) *and* M *as in* (26), *it holds that* $\psi_{0,i}(t) - |e_i(t)| \geq \varepsilon_{0,i}$ *for all* $i \in \{1,\dots,n\}$ *and all* $t \in [0,T)$. Choose $i \in \{1,\dots,n\}$ arbitrarily and note that for $\varepsilon_{0,i}$ as in (29) the Steps 3a-e in the proof of Theorem 3.3 in [10] go through without changes (setting $\gamma = 1$ and $\varepsilon_{0,i} = \varepsilon_0$). Hence the claim of Step 4 holds true.

Step 5: For all $i \in \{1,\dots,n\}$ it is shown that $|\dot{e}_i(\cdot)|$ is uniformly bounded away from the boundary $\psi_{1,i}(\cdot)$; more precisely for positive

$$\varepsilon_{1,i} \quad \leq \quad \min\Big\{ \lambda_{1,i}/2,\, \psi_{1,i}(0) \ -\ |\dot{e}_i(0)|,\, M_\varepsilon \Big\}, \quad (30)$$

with $M_\varepsilon := \frac{\frac{1}{2}\varsigma_{0,i}\varsigma_{1,i}\lambda_{1,i}\varepsilon_{0,i}^2}{\|\psi_{0,i}\|_\infty (M + \|\dot{\psi}_{1,i}\|_\infty)\varepsilon_{0,i}^2 + \|\varsigma_{0,i}\|_\infty^2 \|\psi_{0,i}\|_\infty^2}$, M *as in* (26) *and* $\varepsilon_{0,i}$ *as in* (29), *it holds that* $\psi_{1,i}(t) - |\dot{e}_i(t)| \geq \varepsilon_{1,i}$ *for all* $i \in \{1,\dots,n\}$ *and all* $t \in [0,T)$. Again choose $i \in \{1,\dots,n\}$ arbitrarily and observe that identical arguments as in Step 4 of the proof of Theorem 3.3 in [10] (setting $\gamma = 1$ and $\varepsilon_{1,i} = \varepsilon_1$) show the claim of Step 5.

Step 6: It is shown that Assertions (ii)-(v) hold true.
For M as in (26), $M_{\boldsymbol{z}}$ as in (25), $\varepsilon_{0,i}$ as in (29) and $\varepsilon_{1,i}$ as in (30), $i \in \{1,\dots,n\}$ define

$$\mathfrak{C} := \big\{ (t, (\boldsymbol{\mu}, \boldsymbol{\xi}), \boldsymbol{z}) \in [0,T] \times \mathbb{R}^{2n} \times \mathbb{R}^2 \ \big|\ \forall\, i \in \{0,\dots,n\} : \\ |\mu_i| \leq \psi_{0,i}(t) - \varepsilon_{0,i} \wedge |\xi_i| \leq \psi_{1,i}(t) - \varepsilon_{1,i} \wedge \|\boldsymbol{z}\| \leq M_{\boldsymbol{z}} \big\}.$$

Let $\mathcal{D}$ be as in (21) (see Step 2). If $T < \infty$ then $\mathfrak{C} \subset \mathcal{D}$ and contains the whole graph of the solution $t \mapsto (\boldsymbol{e}(t), \dot{\boldsymbol{e}}(t), \boldsymbol{z}(t))$, which contradicts maximality of the solution. Hence $T = \infty$. Assertion (iii) follows from Step 4 and Step 5. Invoking Lemma 1 (in the Appendix) yields asymptotic stability of (14b), (15), which shows Assertion (iv). Moreover, Step 4 and Step 5 with boundedness of $\boldsymbol{\varsigma}_0(\cdot)$ and $\boldsymbol{\varsigma}_1(\cdot)$ on $\mathbb{R}_{\geq 0}$ imply that $\boldsymbol{K}_0(\cdot)$ and $\boldsymbol{K}_1(\cdot)$ are uniformly bounded on $\mathbb{R}_{\geq 0}$, respectively. Then, from (24), (A_1) and (12), it follows that $\boldsymbol{u}(\cdot)$ is uniformly bounded on $\mathbb{R}_{\geq 0}$. Note that $\boldsymbol{\kappa}(\cdot,\cdot) \in \mathcal{L}^\infty(\mathbb{R}^n \times \mathbb{R}^n; \mathbb{R}^2)$ follows by Assumption (A_7) which with boundedness of $\boldsymbol{z}(\cdot)$ implies $v(\cdot) \in \mathcal{L}^\infty(\mathbb{R}_{\geq 0}; \mathbb{R})$. Hence Assertion (v) is shown. This completes the proof. □

V. Simulation example

In this section, we present simulations as a proof of concept. We apply path-following funnel controller (12) with timing feedback (15) (to be specified later) of a planar elbow-like rigid-link revolute-joint robot with two joints actuated by u_1 and u_2 [Nm], respectively (see Fig. 2). The links are assumed massless and have length l_1 and l_2 [m]. Point masses m_1 and m_2 [kg] are attached to their distal ends, respectively. Control objective is path-following funnel control of joint angles y_1 and y_2 [rad] with *prescribed path accuracy*. The mathematical model of this robot [15, p. 259ff.] is given by

$$\boldsymbol{M}(\boldsymbol{y}(t))\,\ddot{\boldsymbol{y}}(t) + \boldsymbol{C}(\boldsymbol{y}(t),\dot{\boldsymbol{y}}(t))\,\dot{\boldsymbol{y}}(t) + \boldsymbol{g}(\boldsymbol{y}(t)) = \boldsymbol{u}(t) \quad (31)$$

with initial value $(\boldsymbol{y}(0),\dot{\boldsymbol{y}}(0)) = (\boldsymbol{0},\boldsymbol{0})$, inertia matrix

$$\boldsymbol{M}\colon \mathbb{R}^2 \to \mathbb{R}^{2\times 2},\ \boldsymbol{y} \mapsto \boldsymbol{M}(\boldsymbol{y}) := \begin{bmatrix} m_1 l_1^2 + m_2\,(l_1^2 + l_2^2 + 2l_1 l_2\cos(y_2)), & m_2(l_2^2 + l_1 l_2\cos(y_2)) \\ m_2(l_2^2 + l_1 l_2\cos(y_2)), & m_2 l_2^2 \end{bmatrix}, \quad (32)$$

centrifugal and Coriolis force matrix

$$\boldsymbol{C}\colon \mathbb{R}^2\times\mathbb{R}^2 \to \mathbb{R}^{2\times 2},\quad (\boldsymbol{y},\boldsymbol{v}) \mapsto \boldsymbol{C}(\boldsymbol{y},\boldsymbol{v}) := \begin{bmatrix} -2m_2 l_1 l_2\sin(y_2)v_1, & -m_2 l_1 l_2\sin(y_2)v_2 \\ -m_2 l_1 l_2\sin(y_2)v_1, & 0 \end{bmatrix}$$

and gravity vector

$$\boldsymbol{g}\colon \mathbb{R}^2 \to \mathbb{R}^2,\quad \boldsymbol{y} \mapsto \boldsymbol{g}(\boldsymbol{y}) := g\begin{pmatrix} m_1 l_1\cos(y_1) + m_2(l_1\cos(y_1) + l_2\cos(y_1+y_2)) \\ m_2 l_2\cos(y_1+y_2) \end{pmatrix}$$

where $g = 9.81\,[\mathrm{kg\,m^2}]$ is the (rounded) gravity constant. For simplicity, disturbances (and measurement errors, e.g. noise) are neglected. The planar robot satisfies Assumptions (A_1)-(A_5) [16]. The considered path $\theta \mapsto \boldsymbol{p}(\theta) = (\cos(\theta),\ \sin(\theta))^\top$ is a circle in the joint space. The initial condition for the path-parameter state is $\boldsymbol{z}(0) = (\theta_0, 0)^\top$ with $\theta_0 = -1.1\pi$. The aim is to steer the robot to the end of path at $\boldsymbol{p}(0) = (1,0)^\top$. Robot and controller parameters are collected in Tab. I. Note that for controller design solely the inertia matrix must be known. As timing feedback (15), we implement the following error-dependent feedback

$$v(t) = -\alpha(\boldsymbol{e}(t),\dot{\boldsymbol{e}}(t))\boldsymbol{\kappa}^\top\boldsymbol{z}(t) \quad (33)$$

to adjust the timing in (14b). The error-dependent scaling $\alpha : \mathbb{R}^n\times\mathbb{R}^n \to \mathbb{R}_{>0}$ is chosen as

$$\alpha(\boldsymbol{e}(t),\dot{\boldsymbol{e}}(t)) = \frac{\alpha_{\max} + \alpha_{\min}(\|\boldsymbol{e}(t)\| + \|\dot{\boldsymbol{e}}(t)\|)}{\|\boldsymbol{e}(t)\| + \|\dot{\boldsymbol{e}}(t)\| + 1}, \quad (34)$$

where $\alpha_{\min} = 0.82$ and $\alpha_{\max} = 10$ are fixed constants. The intuition behind the choice of $\alpha(\cdot,\cdot)$ in (34) is as follows: For large errors the timing should be decelerated and for small errors it is accelerated again. This is achieved by (34), since $\alpha(\cdot,\cdot)$ is a strictly decreasing function of $\|\boldsymbol{e}\| + \|\dot{\boldsymbol{e}}\|$. Its maximum $\alpha_{\max}$ is attained as $\|\boldsymbol{e}\| + \|\dot{\boldsymbol{e}}\| \to 0$ and, furthermore, it tends to $\alpha_{\min}$ as $\|\boldsymbol{e}\| + \|\dot{\boldsymbol{e}}\| \to \infty$.

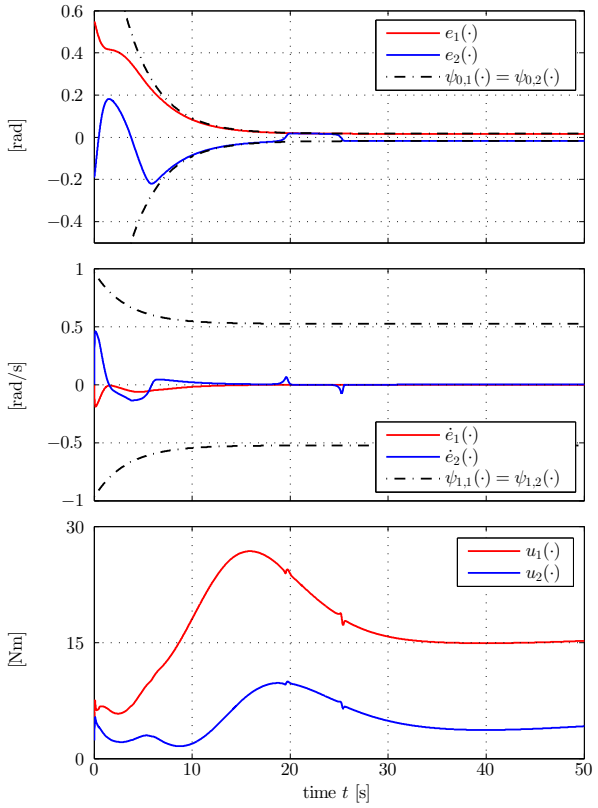

Fig. 3: *Errors* $\boldsymbol{e}(\cdot), \dot{\boldsymbol{e}}(\cdot)$ *and control action* $\boldsymbol{u}(\cdot)$.

For the specific values listed in Tab. I, the product $\alpha(\cdot,\cdot)\boldsymbol{\kappa}$ satisfies (16) with $\underline{\kappa} = \alpha_{\min}\kappa_1 = 0.082$ (i.e. the case $\|\boldsymbol{e}\| + \|\dot{\boldsymbol{e}}\| \to \infty$), $1 + \underline{\kappa} = 1.082 < \alpha_{\min}\kappa_2 = 1.0906$ and $\overline{\kappa} = \alpha_{\max}\kappa_2 = 13.3$ (i.e. the case $\|\boldsymbol{e}\| + \|\dot{\boldsymbol{e}}\| \to 0$).

The simulation results are shown in Figures 3, 4 and 5. As can be seen in Fig. 3, the funnel controller (12) achieves path-following with prescribed transient accuracy for joint positions $y_1(\cdot), y_2(\cdot)$ and joint velocities $\dot{y}_1(\cdot),\ \dot{y}_2(\cdot)$, respectively. Both joint position errors $e_1(\cdot), e_2(\cdot)$ and both joint velocity errors $\dot{e}_1(\cdot),\ \dot{e}_2(\cdot)$ evolve within the performance funnel. The two spikes in the errors and inputs before $t = 20$s and at $t = 25$s are due to the nonlinear coupling of the robot joints. Furthermore, Fig. 4 illustrates the closed-loop dynamics of the path parameter states and the scaling $\alpha(\cdot)$ in the timing feedback (33). Note that the two spikes in the errors before $t = 20$s and at $t = 25$s lead to reduced values of $\alpha(\cdot)$, cf. (34). The behavior of the proposed path-following funnel controller in the $y_1 - y_2$ plane is depicted in Fig. 5. The robot approaches the path and follows it along with prescribed accuracy.

VI. Conclusions

In this paper we have investigated the application of funnel control to path-following problems of rigid-link revolute-joint robotic systems. We showed that under suitable assumptions *prescribed path accuracy* can be guaranteed. Future work will focus on (i) disturbance rejection properties, (ii) robustness of the proposed control scheme in comparison to other path-following approaches and (iii) establishing a feasibility condition in presence of actuator (input) saturation

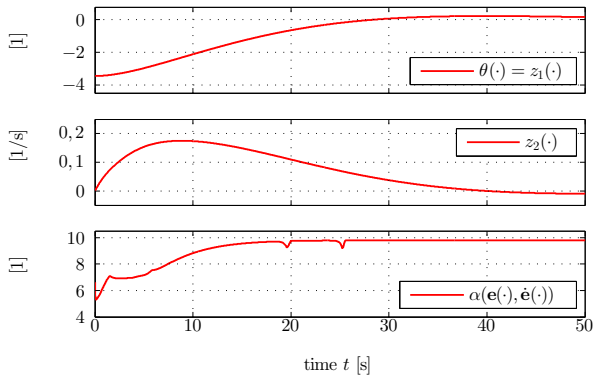

Fig. 4: *Timing states* $\theta(\cdot) = z_1(\cdot), z_2(\cdot)$ *and scaling* $\alpha(\boldsymbol{e}(\cdot), \dot{\boldsymbol{e}}(\cdot))$.

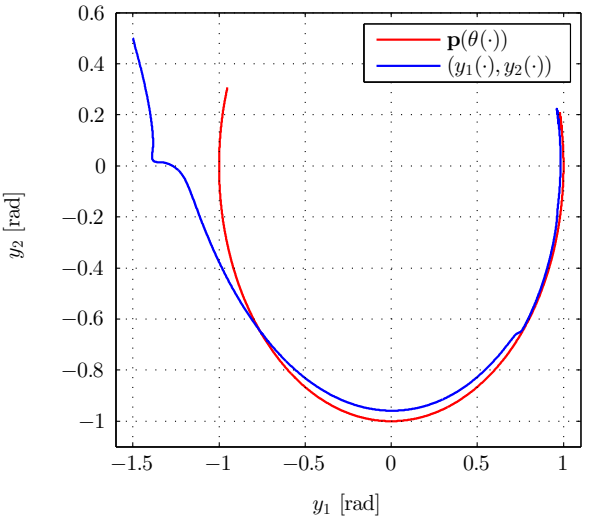

Fig. 5: *Trajectory in the* $y_1 - y_2$ *plane with path* $\boldsymbol{p}(\theta(\cdot))$.

(in the spirit of [11]). Furthermore, it is still an open question how to design the path parameter feedback (15) such that strict forward motion along the path is enforced (e.g. path-following in finite time).

Appendix

Lemma 1 (see Theorem 2.15 in [19])**.** *Let* $\alpha_0(\cdot), \alpha_1(\cdot) \in \mathcal{C}^1(\mathbb{R}_{\geq 0}; \mathbb{R})$ *and* $\underline{\alpha} \geq \overline{\alpha} > 0$ *and consider the planar linear time-varying system given by*

$$\dot{\boldsymbol{z}}(t) = \begin{pmatrix} 0 & 1 \\ -\alpha_0(t) & -\alpha_1(t) \end{pmatrix} \boldsymbol{z}(t), \quad \boldsymbol{z}(0) = \boldsymbol{z}_0 \in \mathbb{R}^2. \quad (35)$$

If (i) $0 < \underline{\alpha} \leq \alpha_0(t) \leq \alpha_1(t) \leq \overline{\alpha}$ *and (ii)* $1 + \underline{\alpha} \leq \alpha_1(t)$ *for all* $t \geq 0$*, then system* (35) *is asymptotically stable.*

References

[1] A. Aguiar, J. Hespanha, and P. Kokotovic, "Path-following for nonminimum phase systems removes performance limitations," *IEEE Trans. Automat. Contr.*, vol. 50, no. 2, pp. 234–239, 2005.

[2] R. Skjetne, T. Fossen, and P. Kokotovic, "Robust output maneuvering for a class of nonlinear systems," *Automatica*, vol. 40, no. 3, pp. 373–383, 2004.

[3] T. Faulwasser, *Optimization-based solutions to constrained trajectory-tracking and path-following problems*. Contributions in Systems Theory and Automatic Control, no. 3, Shaker, Aachen, Germany, 2013.

	data/parametrization
robot (31)	$m_1 = m_2 = 1$ [kg], $l_1 = l_2 = 1$ [m], $(\boldsymbol{y}(0), \dot{\boldsymbol{y}}(0)) = (-1.5, 0.5, 0, 0)$
desired path	$\boldsymbol{p}(\theta) = (\cos(\theta),\ \sin(\theta))^\top$
	$\boldsymbol{z}(0) = (\theta_0, 0)^\top$ with $\theta_0 = -1.1\pi$
initial error	$\boldsymbol{e}(0) = (0.55, -0.19)^\top$ $[\text{rad}]^2$
(MIMO) funnel controller (12)	$\boldsymbol{M}(\boldsymbol{y})$ as in (32), $(\psi_{0,i},\ \psi_{1,i})$, $i \in \{1, 2\}$ as in (10) with $(\Lambda_{0,1},\ \Lambda_{0,2}) = 1.5\,[\text{rad}]^2$, $(\lambda_{0,1},\ \lambda_{0,2}) = \frac{1}{180}(\pi, \pi)$ $[\text{rad}]^2$, $(T_{E,1},\ T_{E,2}) = (3.34,\ 3.34)$ $[\text{s}]^2$, $(\lambda_{1,1},\ \lambda_{1,2}) = \frac{1}{6}(\pi,\ \pi)$ $[\text{rad/s}]^2$, $\boldsymbol{\varsigma}_0(\cdot) = (\psi_{0,1}(\cdot),\ \psi_{0,2}(\cdot))$, $\boldsymbol{\varsigma}_1(\cdot) = 10\,(\psi_{1,1}(\cdot),\ \psi_{1,2}(\cdot))$
timing feedback (33)	$\boldsymbol{\kappa} = (0.1, 1.33)^\top$ $\alpha_{\max} = 10, \alpha_{\min} = 0.82$

TABLE I: *Robot and controller parameters for simulation.*

[4] A. Banaszuk and J. Hauser, "Feedback linearization of transverse dynamics for periodic orbits," *Sys. Contr. Lett.*, vol. 26, no. 2, pp. 95–105, 1995.

[5] C. Nielsen and M. Maggiore, "On local transverse feedback linearization," *SIAM Journal on Control and Optimization*, vol. 47, pp. 2227–2250, 2008.

[6] T. Faulwasser and R. Findeisen, "Nonlinear model predictive path-following control," in *Nonlinear Model Predictive Control - Towards New Challenging Applications* (L. Magni, D. Raimundo, and F. Allgöwer, eds.), Lecture Notes in Control and Information Sciences 384, pp. 335–343, Springer, Berlin, 2009.

[7] T. Faulwasser, J. Matschek, J. Zometa, and R. Findeisen, "Predictive path-following control: Concept and implementation for an industrial robot," in *Proc. of IEEE Multi-Conference on Systems and Control (MSC) 2013, Hyerdabat, India*, 2013.

[8] A. Ilchmann, E. P. Ryan, and C. J. Sangwin, "Tracking with prescribed transient behaviour," *ESAIM: Control, Optimisation and Calculus of Variations*, vol. 7, pp. 471–493, 2002.

[9] A. Ilchmann, E. Ryan, and P. Townsend, "Tracking with prescribed transient behaviour for nonlinear systems of known relative degree," *SIAM Journal on Control and Optimization*, vol. 46, no. 1, pp. 210–230, 2007.

[10] C. M. Hackl, "High-gain adaptive position control," *International Journal of Control*, vol. 84, no. 10, pp. 1695–1716, 2011.

[11] C. M. Hackl, N. Hopfe, A. Ilchmann, M. Mueller, and S. Trenn, "Funnel control for systems with relative degree two," *SIAM Journal on Control and Optimization*, vol. 51, no. 2, pp. 965–995, 2013.

[12] V. Topogonov, *Differential Geometry of Curves and Surfaces - A Concise Guide*. Birkhäuser, Boston, 2006.

[13] R. Kelly, V. S. Davila, and A. Loría, *Control of Robot Manipulators in Joint Space*. London: Springer-Verlag, 2005.

[14] F. Ghorbel, B. Srinivasan, and M. W. Spong, "On the positive definiteness and uniform boundedness of the inertia matrix of robot manipulators," in *Proceedings of the 32nd IEEE Conference on Decision and Control*, (San Antonio, USA), pp. 1103–1108, 1993.

[15] M. W. Spong, S. Hutchinson, and M. Vidyasagar, *Robot Modeling and Control*. New York: John Wiley & Sons, Inc., 2006.

[16] C. M. Hackl and R. M. Kennel, "Position funnel control for rigid revolute joint robotic manipulators with known inertia matrix," in *Proceedings of the 20th Mediterranean Conference on Control and Automation*, (Barcelona, Spain), pp. 615–620, 2012.

[17] D. Hinrichsen and A. Pritchard, *Mathematical Systems Theory I — Modelling, State Space Analysis, Stability and Robustness*. No. 48 in Texts in Applied Mathematics, Berlin: Springer-Verlag, 2005.

[18] A. Isidori, *Nonlinear control systems*. Springer Verlag, 3rd ed., 1995.

[19] L. H. Duc, A. Ilchmann, and S. Siegmund, "On stability of linear time-varying second-order differential equations," *Quarterly of Applied Mathematics*, vol. LXIV, no. 1, pp. 137–151, 2006.